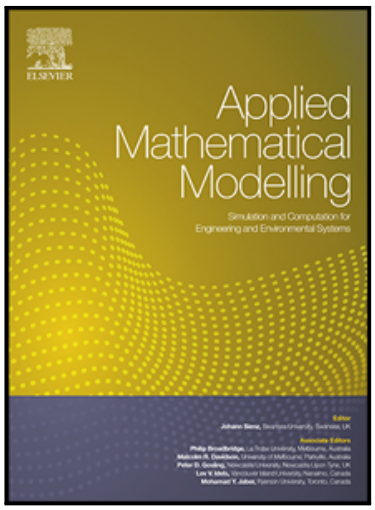

Static and Dynamic Response of CNT Nanobeam using Nonlocal Strain and Velocity Gradient Theory

Hassen M. Ouakad, Sami El-Borgi, S. Mahmoud Mousavi, Michael I. Friswell

PII: S0307-904X(18)30244-0
DOI: 10.1016/j.apm.2018.05.034
Reference: APM 12298

To appear in: *Applied Mathematical Modelling*

Received date: 7 November 2017
Revised date: 27 March 2018
Accepted date: 20 May 2018

Please cite this article as: Hassen M. Ouakad, Sami El-Borgi, S. Mahmoud Mousavi, Michael I. Friswell, Static and Dynamic Response of CNT Nanobeam using Nonlocal Strain and Velocity Gradient Theory, *Applied Mathematical Modelling* (2018), doi: 10.1016/j.apm.2018.05.034

Highlights

- We study length-scale effect on response of an actuated CNT nano-actuator using a nonlocal strain-Velocity gradient theory.
- The nano-actuator is modeled as a Euler-Bernoulli beam which accounts for von-Karman strain and electric actuating forcing.
- Three length-scale parameters are included, namely a nonlocal, a strain gradient, and a velocity gradient parameter.
- Equation of motion and boundary conditions are derived using Hamilton's principle and DQM was used to discretize the problem.
- The main objective is to study the effect of length-scale parameters on nonlinear vibrational response of the nano-actuator.

Static and Dynamic Response of CNT Nanobeam using Nonlocal Strain and Velocity Gradient Theory

Hassen M. Ouakad[a], **Sami El-Borgi**[b,1], **S. Mahmoud Mousavi**[c], **Michael I. Friswell**[d]

[a] Mechanical Engineering Department, King Fahd University of Petroleum and Minerals, P.O. Box 31261, Dhahran, Kingdom of Saudi Arabia.
[b] Mechanical Engineering Program, Texas A&M University at Qatar, P.O. Box 23874, Education City, Doha, Qatar.
[c] Department of Engineering and Physics, Karlstad University, 65188 Karlstad, Sweden.
[d] Swansea University, Bay Campus, Fabian Way, Swansea SA1 8EN, UK.

Abstract

This paper examines the length-scale effect on the nonlinear response of an electrically actuated Carbon Nanotube (CNT) based nano-actuator using a nonlocal strain and velocity gradient (NSVG) theory. The nano-actuator is modeled within the framework of a doubly-clamped Euler - Bernoulli beam which accounts for the nonlinear von-Karman strain and the electric actuating forcing. The NSVG theory includes three length-scale parameters which describe two completely different size-dependent phenomena, namely, the inter-atomic long-range force and the nano-structure deformation mechanisms. Hamilton's principle is employed to obtain the equation of motion of the nonlinear nanobeam in addition to its respective classical and non-classical boundary conditions. The differential quadrature method (DQM) is used to discretize the governing equations. The key aim of this research is to numerically investigate the influence of the nonlocal parameter and the strain and velocity gradient parameters on the nonlinear structural behavior of the carbon nanotube based nanobeam. It is found that these three length-scale parameters can largely impact the performance of the CNT based nano-actuator and qualitatively alter its resultant response. The main goal of this investigation is to understand the highly nonlinear response of these miniature structures to improve their overall performance.
Keywords: Carbon Nanotube (CNT) Euler-Bernoulli nanobeam; Nonlocal strain and velocity gradient theory; Material length scales; Differential Quadrature Method (DQM); Static and eigenvalue problem.

1 Introduction

Carbon nanotubes (CNTs) are considered as mechanical building blocks at the nano-scale thanks to their outstanding characteristics including thermal, mechanical, electrical and chemical properties. CNTs have received widespread interest of researchers from many disciplines, including material science, engineering, chemistry, and physics and in applications involving nano-electronics, nanosensors, and nanodevices [1]-[6]. Therefore, an extensive study of the structural behavior of CNTs under various conditions is a fundamental issue in any nano-scale investigation.

[1]Corresponding author. Tel.: +974 4423 0674, e-mail: sami.el_borgi@qatar.tamu.edu (Sami El-Borgi).

The existence of size-dependency of CNTs was confirmed experimentally at the nanoscale [7]. Recently, several models that include the effect of material length scales have been developed to predict the size-dependent behavior of nanobeams. These include Eringen's nonlocal elasticity theory [7]–[10], modified couple stress theory of Mindlin [11], Koiter [12], and Toupin [13] and the strain gradient theory [14]–[16].

Unlike classical continuum mechanics, nonlocal theories assume that the stress at a point is not a function of the strain at that point but is a function of the strains in its neighborhood [7]–[10]. These theories account for the inter-atomic long-range force but do not consider the microstructure deformation mechanism as in the case of classical elasticity [17]. Nonlocal elastic models can only model nanostructures exhibiting softening behavior which indicates that "smaller is more compliant" [18]. On the other hand, the gradient elasticity theory considers only the higher-order microstructure deformation mechanism without accounting for any inter-atomic long-range force. Furthermore, gradient elasticity theory can only model nanostructures exhibiting hardening behavior which indicates that "smaller is stiffer" [18]. Therefore, nonlocal elasticity and strain gradient theories represent two different size-dependent behaviors and combining both theories allows the modeling of nanostructures exhibiting at the same time hardening and softening behavior. Tian et al. [19] were able to show experimentally on certain nanostructures stiffness enhancement and softening effects, indicating the need for a unique theory capable of capturing both size-dependent stiffness-softening and hardening phenomena. Recently, a number of researchers employed the combined nonlocal strain gradient theory to investigate the effects of the two length-scale parameters (ie, the nonlocal and strain gradient parameter) on the behavior of nano/micro-structures [17]–[18],[20]–[21].

With the recent development in size-dependent continuum mechanics theories, there has been more focus on investigating the vibration response of CNT nanobeams using a number of numerical and analytical techniques and size dependent models. Many studies investigated the linear free vibration of CNT beams. Thongyothee et al. [22] examined the linear and free vibration of SWCNTs while taking into consideration the effect of small length scale based on the nonlocal elasticity theory. Kiani [23] investigated the vibrational behavior of simply supported inclined SWCNTs conveying viscous fluids flow using nonlocal Rayleigh beam model. On the other hand, Xu and Deng [24] presented variational methods to investigate the buckling and free vibration of CNT beams using the strain gradient theory. Li et al. [25] studied numerically the longitudinal nonlinear vibration of nanorods employing the nonlocal strain gradient theory. De Rosa and Lippiello [26] investigated analytically the nonlocal vibration analysis of single-walled carbon nanotube Timoshenko beam used in mass-sensor applications.

The aforementioned studies focused on linear vibration problems of CNT nanobeams. Few investigations took into consideration the geometric nonlinearity associated with vibration of CNT nanobeams. Ke and his co-authors [31]–[33] made the first attempt to study the nonlinear vibration of the single-walled and double-walled carbon nanotubes based on nonlocal Timoshenko beam theory. Ke et al. [31] investigated the nonlinear free vibration problem of functionally graded nanocomposite beams reinforced by single-walled carbon nanotubes (SWCNTs) considering Timoshenko beam theory and von Karman geometric nonlinearity. In another paper, Yang et al. [32] and Ke et al. [33] investigated, respectively, the nonlinear free vibration response of embedded single-walled and double-walled carbon nanotubes based on nonlocal Timoshenko beam theory. The aforementioned studies by Ke and co-authors concluded that the nonlocal parameter has an insignificant effect on the nonlinear mode shape but can considerably change the linear and nonlinear frequen-

cies. Ansari et al. [27] employed the strain gradient elasticity theory to study the torsional vibration behavior of single-walled carbon nanotubes modelled as a Euler-Bernoulli beam and the resulting problem was solved numerically using the Differential Quadrature Method (DQM). Fakhrabadi et al. [28] investigated numerically the nonlinear free/forced vibration of CNT under DC electrostatic load while assuming the so-called modified couple stress theory. Mehdipour et al. [29] considered the nonlocal nonlinear vibration problem of an electrostatically actuated cantilevered CNT based bio-mass sensor with a mass attached to its free end. Fang et al. [30] analyzed the nonlinear vibration response of double-walled carbon nanotubes based on nonlocal elasticity theory. Recently, Rahmanian et al. [34] studied the free nonlinear vibration of single walled carbon nanotubes using nonlocal elasticity beam and shell models.

Another type of nonlinearity is caused by the electrostatic force in electrically actuated CNT beams. Using the finite element method, Ribeiro [35] studied numerically the nonlocal nonlinear structural behavior of electrically actuated carbon nanotube based nano-actuators. Yang et al. [36] investigated the dynamic pull-in instability of electrically carbon nanotube based nano-actuator using the nonlocal strain gradient theory and the solution to the governing equations was obtained analytically using the Homotopy Perturbation Method.

Size effect appears when the internal structure is not negligible in comparison to the structural dimension. In order to improve the continuum model to capture this feature, elastodynamic formulation should be generalized in a constitutive level. This generalization, in principle cannot be limited to the stress-strain constitutive equation, and both strain and kinetic energy should be generalized [37]–[38]. Then, it is only a matter of scale to see the effect of the static and/or kinetic internal length scale in the behavior of the structure. A limited number of investigators accounted for velocity gradient effect in studying vibration of different structural elements. Guo et al. [39] investigated the torsional free vibration linear response of a carbon nanotube using a combined nonlocal with strain and velocity gradient theory. This study concluded that the effect of including velocity gradient weakens the nanotube's torsional rigidity and has a larger influence on higher-order frequencies than on lower-order frequencies. Fernandes et al. [40] considered the nonlinear vibration problem of a carbon nanotube bar embedded in an elastic medium using the strain and velocity gradient theory. In another study, Fernandes et al. [41] examined the nonlinear free and forced vibration response of a microbeam using finite strain and velocity gradient theory. Finally, El-Borgi et al. [42] studied the torsional vibration of viscoelastic rods using nonlocal strain and velocity gradient theory.

To the best of the authors knowledge, it can be concluded from the literature review that, with the exception of the work of Yang et al. [36], all researchers have focused their attention on studying the nonlinear dynamic behavior of electrically actuated CNT based nano-actuator using either the nonlocal theory or the strain gradient theory / modified coupled stress theory which account, respectively, for the inter-atomic long-range force and the microstructure deformation mechanism. Additionally, the generalization of the strain energy with strain gradient should be incorporated with the generalization of the kinetic energy with velocity gradient. To fill these gaps in the literature, the novelty of this study consists of combining nonlocal strain and velocity gradient theories to capture the size effects in the vibration response of a CNT nanobeam with nonlinearities due to von Kármán nonlinear strains and electrostatic forcing. As a result, both inter-atomic long-range force and the microstructure deformation mechanism will be considered in the proposed theory. It is noted that Yang et al. [36] analyzed the dynamic pull-in of functionally graded nanotubes

reinforced nano-actuator without considering the velocity gradient. In this article, adopting a different solution approach, in that the velocity gradient has been taken into account. Hamilton's principle is used to derive the equation of motion and the associated boundary conditions of the nanobeam. The differential quadrature method (DQM) is then employed to discretize the nonlinear equation of motion of the nano-actuator and the nonlinear response is subsequently solved.

This paper is arranged as follows. Following this introduction, the proposed nonlocal strain gradient theory is summarized in Section 2. The equations of motion for a size-dependent Euler-Bernoulli CNT nanobeam employing the nonlocal strain and velocity gradient theory along with von Kármán and electrostatic forcing nonlinearities are derived in Section 3. The model discretization using the differential quadrature method is presented in Section 4. Numerical results are presented and discussed in Section 5. Finally, the main contributions and conclusions are provided in Section 6.

2 Nonlocal Strain Gradient Theory

In this section, we formulate the static and dynamic behavior of an electrically actuated carbon nanotube resonator taking into consideration the nonlocal theory as well as both the strain and velocity gradient theories. The considered boundary conditions for the carbon nanotube (CNT) is a clamped-clamped beam, Fig. 1. The CNT is actuated by an electrode underneath it with a gap width d. The CNT is modeled as an Euler-Bernoulli beam of radius $\tilde{R}$, and length L. This beam has a cross-sectional area $A = \pi\tilde{R}^2$, and an area moment of inertia of $I = \pi\tilde{R}^4/4$. The CNT is assumed to have a Young's modulus $E = 1$ TPa and a density $\rho = 1.35$ g/cm^3 [43].

According to the non-gradient nonlocal elastic stress field theory [7, 44], the nonlocal stress at a reference point $\mathbf{x}$ depends not only on the strain $\boldsymbol{\varepsilon}$ at that location but on the strains at all other points within the domain V. Hence, the nonlocal internal energy density potential U_0 can be written as

$$U_0\left(\varepsilon_{ij}, \varepsilon_{ij}, \alpha_0\right) = \frac{1}{2}\varepsilon_{ij} C_{ijkl} \int_V \alpha_0\left(\left|\mathbf{x}-\mathbf{x}'\right|, e_0 a\right) \varepsilon_{kl} dV \tag{1}$$

The extended Eringen's model including the nonlocality of higher-order strain gradients $\varepsilon_{ij,k}$ reads

$$U_0(\varepsilon_{ij}, \varepsilon_{ij}, \alpha_0; \varepsilon_{ij,m}, \varepsilon_{ij,m}, \alpha_1) = \frac{1}{2}\varepsilon_{ij} C_{ijkl} \int_V \alpha_0\left(\left|\mathbf{x}-\mathbf{x}'\right|, e_0 a\right) \varepsilon_{kl} dV + \frac{l_s^2}{2}\varepsilon_{ij,m} C_{ijkl} \int_V \alpha_1\left(\left|\mathbf{x}-\mathbf{x}'\right|, e_1 a\right) \varepsilon_{kl,m} dV = \frac{1}{2}\int_V \left(\sigma_{ij}\varepsilon_{ij} + \sigma_{ijm}^{(1)}\varepsilon_{ij,m}\right) dV \tag{2}$$

where $\sigma_{ij} = C_{ijkl}\int_V \alpha_0\left(\left|\mathbf{x}-\mathbf{x}'\right|, e_0 a\right)\varepsilon_{kl} dV$ and $\sigma_{ijm}^{(1)} = l_s^2 C_{ijkl}\int_V \alpha_1\left(\left|\mathbf{x}-\mathbf{x}'\right|, e_1 a\right)\varepsilon_{kl,m} dV$ are, respectively, the nonlocal stress tensor and the higher-order nonlocal stress tensor. Here, $e_0 a$ and $e_1 a$ are nonlocal parameters representing the significance of the inter-atomic long-range force and l_s is the material length-scale parameter associated with the strain gradient. The nonlocal strain gradient theory [45] states that the total stress tensor t_{ij} can account for not only the local stress tensor σ_{ij}, but also the higher-order nonlocal stress tensor $\nabla\sigma_{ijm}^{(1)}$, as follows:

$$t_{ij} = \sigma_{ij} - \nabla \sigma^{(1)}_{ijm} \tag{3}$$

Based on Eringen [8], the nonlocal parameters are assumed to be $e_0 a = e_1 a = ea$, which reduces the general constitutive relations of the Nonlocal Strain Gradient (NLG) theory to the following form:

$$\left[1 - (ea)^2 \nabla^2\right] t_{xx} = \left(1 - l_s^2 \nabla^2\right) E(z) \varepsilon_{xx} \tag{4a}$$

$$\left[1 - (ea)^2 \nabla^2\right] t_{xz} = \left(1 - l_s^2 \nabla^2\right) G(z) \gamma_{xz} \tag{4b}$$

where $G(z)$ is the shear modulus, t_{xx} is the axial normal stress, ε_{xx} is the axial strain, t_{xz} is the shear stress and γ_{xz} is the shear strain. Such model combines the Eringen's nonlocal elasticity theory and strain gradient theory. In the limiting cases:
1. Setting $l_s = 0$, Equations (4a) and (4b) reduce to

$$\left[1 - (ea)^2 \nabla^2\right] t_{xx} = E(z) \varepsilon_{xx} \tag{5a}$$

$$\left[1 - (ea)^2 \nabla^2\right] t_{xz} = G(z) \gamma_{xz} \tag{5b}$$

which corresponds to Eringen's nonlocal theory.
2. Setting $ea = 0$, Equations (4a) and (4b) reduce to

$$t_{xx} = \left(1 - l_s^2 \nabla^2\right) E(z) \varepsilon_{xx} \tag{6a}$$

$$t_{xz} = \left(1 - l_s^2 \nabla^2\right) G(z) \gamma_{xz} \tag{6b}$$

which is the strain gradient theory with $l_2 = l_s$, $l_0 = l_1 = 0$.

Fernández-Sáez et al. [46] and Romano et al. [47], and the references therein, highlighted a paradox in the transformation from the integral form of the nonlocal model to the differential form for beam bending problems with an exponential nonlocal kernel. They showed that the transformation implied a relationship between the bending moment and the spatial derivative of the bending moment at the boundaries that must be satisfied. This means that the bending moment obtained from the solution to the differential equation should be checked to ensure the obtained solution is also a solution to the integral form of the equation. This is readily done for problems with displacement type boundary conditions, since the bending moment will be the solution of a second order differential equation, and the constants of integration can be used to satisfy the bending moment boundary conditions. However, it should also be recognised that the nonlocal model in integral form is unable to model detailed local effects at boundaries, and hence there are always likely to be discrepancies between the actual and simulated bending moment at the boundary. Given that these discrepancies at the boundaries are always likely to be present whichever model used, here the differential form of the equations is used.

3 Equations of Motion of Size-Dependent CNT Nanobeams

Assuming an Euler-Bernoulli beam model, the carbon nanotube displacement field can be expressed as

$$u_1 = u\left(x,t\right) - zw\left(x,t\right)_{,x}, \quad u_2 = 0, \quad u_3 = w\left(x,t\right) \tag{7}$$

Considering von-Karman nonlinearity for mid-plane stretching effect, the first order nonlinear strain-displacement relation is given by:

$$\varepsilon_{xx} = u_{,x} + \frac{1}{2}w_{,x}^2 - zw_{,xx}, \quad \varepsilon_{xy} = \varepsilon_{xz} = \varepsilon_{yz} = \varepsilon_{yy} = \varepsilon_{zz} = 0 \tag{8}$$

Therefore, the variation of the total strain energy can be expressed as

$$\delta U_t = \int\limits_V \left(\sigma_{xx}\delta\varepsilon_{xx} + \sigma_{xxx}^{(1)}\nabla\delta\varepsilon_{xx}\right)dV = \int\limits_V \left(\sigma_{xx} - \nabla\sigma_{xxx}^{(1)}\right)\delta\varepsilon_{xx}dV +$$
$$\left[\int\limits_{A_b} \sigma_{xxx}^{(1)}\delta\varepsilon_{xx}dA_b\right]_0^L = \int\limits_V t_{xx}\delta\varepsilon_{xx}dV + + \left[\int\limits_{A_b} \sigma_{xxx}^{(1)}\delta\varepsilon_{xx}dA_b\right]_0^L \tag{9}$$

Substituting Eq. (8) into (9) yields

$$\delta U_t = \int\limits_V t_{xx}\delta\left(u_{,x} + \frac{1}{2}w_{,x}^2 - zw_{,xx}\right)dV + \left[\int\limits_{A_b} \sigma_{xxx}^{(1)}\delta\left(u_{,x} + \frac{1}{2}w_{,x}^2 - zw_{,xx}\right)dA_b\right]_0^L =$$
$$\int\limits_V \left(t_{xx}\delta u_{,x} + t_{xx}w_{,x}\delta w_{,x} - zt_{xx}\delta w_{,xx}\right)dV +$$
$$\left[\int\limits_{A_b} \left(\sigma_{xxx}^{(1)}\delta u_{,x} + \sigma_{xxx}^{(1)}w_{,x}\delta w_{,x} - z\sigma_{xxx}^{(1)}\delta w_{,xx}\right)dA_b\right]_0^L =$$
$$\int\limits_V \left(t_{xx}dA_b\delta u_{,x} + t_{xx}w_{,x}dA_b\delta w_{,x} - zt_{xx}dA_b\delta w_{,xx}\right)dx +$$
$$\left[N^{(1)}\delta u_{,x} + N^{(1)}w_{,x}\delta w_{,x} - M^{(1)}\delta w_{,xx}\right]_0^L =$$
$$\int_0^L \left(N\delta u_{,x} + Nw_{,x}\delta w_{,x} - M\delta w_{,xx}\right)dx + \left[N^{(1)}\delta u_{,x} + N^{(1)}w_{,x}\delta w_{,x} - M^{(1)}\delta w_{,xx}\right]_0^L \tag{10}$$

where,

$$N = \int\limits_{A_b} t_{xx}dA_b, \quad M = \int\limits_{A_b} zt_{xx}dA_b, \quad N^{(1)} = \int\limits_{A_b} \sigma_{xxx}^{(1)}dA_b, \quad M^{(1)} = \int\limits_{A_b} z\sigma_{xxx}^{(1)}dA_b \tag{11}$$

Considering the constitutive relation (3) and (11), the moment and the axial force can be written as follows:

$$M(x,t) = \int_{A_b} z t_{xx} dA_b = \int_{A_b} z \left(\sigma_{xx} - \sigma^{(1)}_{xxx,x}\right) dA_b = M^{(0)} - M^{(1)}_{,x} \tag{12}$$

$$N(x,t) = \int_{A_b} t_{xx} dA_b = \int_{A_b} \left(\sigma_{xx} - \sigma^{(1)}_{xxx,x}\right) dA_b = N^{(0)} - N^{(1)}_{,x} \tag{13}$$

in which

$$M^{(0)} = \int_{A_b} z\sigma_{xx} dA_b, \quad N^{(0)} = \int_{A_b} \sigma_{xx} dA_b \tag{14}$$

Substituting the general constitutive relations (4a) and (4b) and the strain-displacement relationships (8) into Eqs. (12), (13) and (14) yields the following expressions:

$$M(x,t) = (ea)^2 M_{,xx} + EI\left(1 - l_s^2 \frac{\partial^2}{\partial x^2}\right) w_{,xx} \tag{15}$$

$$N(x,t) = (ea)^2 N_{,xx} + EA\left(1 - l_s^2 \frac{\partial^2}{\partial x^2}\right)\left[u_{,x} + \frac{1}{2} w_{,x}^2\right] \tag{16}$$

Based on Mindlin derivations [48] related to the kinetic energy in the gradient elasticity theory, kinematics quantities should be distinguished on the microscale structure. He suggested a generalized kinetic energy in the gradient theory as

$$K = \frac{1}{2}\rho u_{i,t} u_{i,t} + \frac{1}{2}\rho l_k^2 u_{i,jt} u_{i,jt} \tag{17}$$

where ρ is the mass density, l_k is the kinetic material length-scale parameter associated with the velocity gradient and the index t denotes the time derivative. Therefore, the kinetic energy K_t in the region V occupied by elastically deformed material (at time t) can be expressed as:

$$K_t = \int_V K dV = \frac{1}{2}\int_V \rho\left(u_{i,t} u_{i,t} + l_k^2 u_{i,jt} u_{i,jt}\right) dV \tag{18}$$

and its variation is

$$\delta K_t = \int_V \rho\left(u_{i,t}\delta u_{i,t} + l_k^2 u_{i,jt}\delta u_{i,jt}\right) dV \tag{19}$$

Using the Euler-Bernoulli beam model and the displacement field given by Eq. (7), the kinetic energy can be written as follows:

$$K_t = \frac{1}{2}\rho \int_{x=0}^{x=L} \int_A \left[u_{1,t}^2 + u_{3,t}^2 + l_k^2\left(u_{1,xt}^2 + u_{1,zt}^2 + u_{3,xt}^2\right)\right] dA dx \tag{20}$$

For thin beams (valid for CNT), the kinetic energy due to rotation may be neglected when compared to the other term, i.e, $u_{1,xt}^2 \approx 0$ amd $u_{3,zt}^2 \approx 0$. Therefore, the first variation of the kinetic energy can then be written as:

$$\delta K_t = \rho \int_{x=0}^{x=L} \int_A \left[z^2 w_{,xt} \delta w_{,xt} + w_{,t} \delta w_{,t} + u_{,t} \delta u_{,t} - 2z(w_{,xt} \delta u_{,t} + u_{,t} \delta w_{,xt}) \right] dA dx$$
$$+ \rho l_k^2 \int_{x=0}^{x=L} \int_A \left[\left(z^2 w_{,xxt} \delta w_{,xxt} + 2 w_{,xt} \delta w_{,xt} \right) \right] dA dx =$$
$$\rho I \int_{x=0}^{x=L} w_{,xt} \delta w_{,xt} dx + \rho A \int_{x=0}^{x=L} (w_{,t} \delta w_{,t} + u_{,t} \delta u_{,t}) dx +$$
$$\rho l_k^2 I \int_{x=0}^{x=L} w_{,xxt} \delta w_{,xxt} dx + 2\rho l_k^2 A \int_{x=0}^{x=L} w_{,xt} \delta w_{,xt} dx \tag{21}$$

Finally, the variation of the work of external forces takes the form

$$\delta W_t = \int_{x=0}^{x=L} \left(F_{electric}(x,t) - c w_{,t} \right) \delta w dx \tag{22}$$

In such systems, the state is described by using continuous functions of space and time. The extended Hamilton Principle is given by

$$\int_{t_1}^{t_2} \delta L_t dt = \int_{t_1}^{t_2} \left(\delta K_t - \delta U_t + \delta W_t \right) dt = 0 \tag{23}$$

where L_t is the Lagrangian, K_t is the kinetic energy, U_t is the elastic energy, W_t is the nonconservative work done by external loads on the system, and t_1, t_2 are the initial and final times. Substituting the expressions for δU_t, δK_t and δW_t, from Eqs. (10), (21) and (22) into Eq. (23), carrying out integration-by parts over time and space, and assuming that the variations vanish at time t_1 and t_2 results in the following equations of motion:

$$N_{,x} - \rho A u_{,tt} = 0 \tag{24}$$

$$-\left(N w_{,x}\right)_{,x} - M_{,xx} - \rho A w_{,tt} - c w_{,t} - \rho I w_{,xxtt} - 2 l_k^2 \rho A w_{,xxtt} + l_k^2 \rho I w_{,xxxxtt} + F_{electric}(x,t) = 0 \tag{25}$$

subjected to the classical boundary conditions

$$N \quad \text{or} \quad u \qquad \text{evaluated at} \quad x = 0, L \tag{26a}$$
$$M \quad \text{or} \quad w_{,x} \qquad \text{evaluated at} \quad x = 0, L \tag{26b}$$

and the following non-classical boundary conditions:

$$N^{(1)} \quad \text{or} \quad u_{,x} \qquad \text{evaluated at} \quad x = 0, L \tag{27a}$$
$$M^{(1)} \quad \text{or} \quad w_{,xx} \qquad \text{evaluated at} \quad x = 0, L \tag{27b}$$

Knowing that in such flexible structure configuration, the dynamics in the axial direction is obviously less dominant as compared to its bending dynamics, and therefore the inertia term in Eq. (24) can be neglected, i.e., $u_{,tt} \approx 0$, hence one obtains

$$N_{,x} = 0 \rightarrow N(x,t) = C(t) \tag{28}$$

where C is a constant function of time. Substituting (28) into (16), the axial force function $N(x,t)$ is reduced to the following form:

$$N(x,t) = C(t) = (ea)^2 \underbrace{N_{,xx}}_{=0} + EA\left(1 - l_s^2 \frac{\partial^2}{\partial x^2}\right)\left[u_{,x} + \frac{1}{2}w_{,x}^2\right] =$$
$$EA\left[u_{,x} + \frac{1}{2}w_{,x}^2\right] - \frac{\partial}{\partial x}\left(EAl_s^2\left[u_{,xx} + w_{,x}w_{,xx}\right]\right) \tag{29}$$

Using the relationship in Eq. (13), one obtains the following explicit expressions:

$$N^{(0)} = EA\left[u_{,x} + \frac{1}{2}w_{,x}^2\right] \tag{30a}$$
$$N^{(1)} = EAl_s^2\left[u_{,xx} + w_{,x}w_{,xx}\right] \tag{30b}$$

Then, substituting (30a) and (30b) into (16) and in light of (28), one obtains

$$C(t) = EA\left[u_{,x} + \frac{1}{2}w_{,x}^2\right] - N_{,x}^{(1)} \tag{31}$$

Now, in the case of fixed-fixed beams, the axial displacements and the non-classical axial load are equal to zero at the beam boundaries, i.e:

$$u(x = 0, t) = u(x = L, t) = 0 \tag{32a}$$
$$N^{(1)}(x = 0, t) = N^{(1)}(x = L, t) = 0 \tag{32b}$$

Integrating both sides of Eq. (31) from 0 to L and using (30a), (30b) and (31), the axial normal force reduces to the following form:

$$N(x,t) = C(t) = \frac{EA}{2L}\left[\int_{x=0}^{x=L} w_{,x}^2 dx\right] \tag{33}$$

In view of the size-dependent equilibrium Eqs. (25) and (26), the expression of the moment (15) can be written as follows:

$$M(x,t) = (ea)^2\left[\rho A w_{,tt} - \rho A w_{,xxtt} - \frac{EA}{2L}\left(\int_{x=0}^{x=L} w_{,x}^2 dx\right) w_{,xx} - F_{electric}(x,t)\right] -$$
$$EI\left(1 - l_s^2 \frac{\partial^2}{\partial x^2}\right) w_{,xxx} \tag{34}$$

Finally, using (25), (26), (33) and (34) yields the following size-dependent nonlinear equation of motion for a CNT clamped-clamped nanobeam:

$$\left(1-(ea)^2\frac{\partial^2}{\partial x^2}\right)\left[\rho A w_{,tt}-\rho I w_{,xxtt}+c w_{,t}-\left(\frac{EA}{2L}\int\limits_{x=0}^{x=L} w_{,x}^2 dx\right)w_{,xx}-F_{electric}(x,t)\right]=$$
$$\rho l_k^2\left(2A w_{,xxtt}-I w_{,xxxxtt}\right)-\left(1-l_s^2\frac{\partial^2}{\partial x^2}\right)EI w_{,xxxx} \tag{35}$$

subjected to the following boundary conditions:

$$\begin{aligned} &w(x=0,t)=w(x=L,t)=0\\ &w_{,x}(x=0,t)=w_{,x}(x=L,t)=0\\ &w_{,xx}(x=0,t)=w_{,xx}(x=L,t)=0 \end{aligned} \tag{36}$$

The electric force of a CNT clamped-clamped based actuator can be written as

$$F_{electric}(x,t)=\frac{\pi\varepsilon_0 V^2}{\sqrt{(d-w)\left(d-w+2\tilde{R}\right)}\left(\cosh^{-1}\left(1+\frac{d-w}{\tilde{R}}\right)\right)^2} \tag{37}$$

Using the following non-dimensional parameters:

$$\hat{w}=\frac{w}{d},\hat{x}=\frac{x}{L},\hat{t}=\frac{t}{T} \tag{38}$$

where T is a time constant defined by $T=\sqrt{\rho AL^4/EI}$. Dropping the hats, the nondimensional equations of motion and associated boundary conditions for the clamped-clamped carbon nanotube beam can be written, respectively, as

$$\left(1-\mu_s\frac{\partial^2}{\partial x^2}\right)\frac{\partial^4 w}{\partial x^4}+$$
$$\left(1-\mu_0\frac{\partial^2}{\partial x^2}\right)\left(\frac{\partial^2 w}{\partial t^2}+\alpha_d\frac{\partial w}{\partial t}-\alpha_r\frac{\partial^4 w}{\partial x^2\partial t^2}-\alpha_s\left(\int\limits_0^1\left(\frac{\partial w}{\partial x}\right)^2 dx\right)\frac{\partial^2 w}{\partial x^2}-\alpha_e\Gamma(w)\right)=$$
$$\mu_k\left(2\frac{\partial^4 w}{\partial x^2\partial t^2}-\alpha_r\frac{\partial^6 w}{\partial x^4\partial t^2}\right) \tag{39}$$

$$\begin{aligned} &w(x=0,t)=w(x=L,t)=0\\ &w_{,x}(x=0,t)=w_{,x}(x=L,t)=0\\ &w_{,xx}(x=0,t)=w_{,xx}(x=L,t)=0 \end{aligned} \tag{40}$$

where

$$\alpha_s=\frac{Ad^2}{2I},\quad \alpha_e=\frac{\pi\varepsilon_0 L^4}{EId^2},\quad \alpha_r=\frac{I}{AL^2},\quad \alpha_d=\tilde{c}\frac{L^4}{EI} \tag{41a}$$

$$\mu_0=\left(\frac{ea}{L}\right)^2,\quad \mu_s=\left(\frac{l_s}{L}\right)^2,\quad \mu_k=\left(\frac{l_k}{L}\right)^2,\quad R=\frac{\tilde{R}}{d} \tag{41b}$$

and

$$\Gamma(w) = \frac{V^2}{\sqrt{(1-w)(1-w+2R)}\left(\cosh^{-1}\left(1+\frac{1-w}{R}\right)\right)^2} \tag{42}$$

4 Differential Quadrature Method (DQM)

Due to the complexity of the governing equation Eq. (39) of the clamped-clamped carbon nanotube, it is indispensable to use a numerical method to simulate its response. In this work, we propose the use of Differential Quadrature Method (DQM). Various problems in structural mechanics have been solved successfully with the aid of DQM, and it has been shown that it leads to more accurate results at a lower computational cost.

4.1 General DQM Formulation

The basic concept of the differential quadrature (DQM) based discretization Technique is to estimate the derivative of the required CNT nonlinear response function $w(x)$ with respect to the space variable x at a given random sample of points. The obtained differential equation will formerly be converted into a set of algebraic equations for the static response and into a set of ordinary differential equations (ODEs) for the dynamic response. For the accuracy of the numerical results, the following grid point distribution is used [49]:

$$x_i = \frac{1}{2}\left[1-\cos\left(\frac{i-1}{n-1}\pi\right)\right], i = 1, 2, ...n \tag{43}$$

Such distribution was found to yield more accurate results and obtain the convergence of the solution with a smaller number of grid points in comparison with other sampling schemes [49]. Consequently, for a dimensionless variable x defined in the domain (0,1) and using n discretization points over the domain, the p^{th}-order derivative of $w(x)$ at $x = x_i$ can be expressed as

$$\left.\frac{\partial^p w}{\partial x^p}\right|_{x=x_i} = \sum_{j=1}^{n} D_{ij}^{(p)} w_j \tag{44}$$

where, as an example, the off-diagonal terms of the weighting coefficient matrix of the first order derivative are calculated as follows:

$$D_{ij}^{(p=1)} = \frac{\prod_{k=1,k\neq i}^{n}(x_i - x_k)}{(x_i - x_j)\prod_{k=1,k\neq j}^{n}(x_j - x_k)} \qquad i,j = 1,2,...,n \quad i \neq j \tag{45}$$

On the other hand, the remaining higher-order derivative weighting coefficient matrices are computed on the following recurrence relationship:

$$\begin{cases} A_{ij}^{(p)} = p\left[A_{ii}^{p-1}A_{ij}^{1} - \frac{A_{ij}^{p-1}}{x_i - x_j}\right] & i,j = 1,2,...,n \quad i \neq j \quad , 2 \leq p \leq n-1 \\ A_{ii}^{(p)} = -\sum_{k=1,k\neq i}^{n} A_{ik}^{p} & i = 1,2,...,n \;\; 1 \leq p \leq n-1 \end{cases} \tag{46}$$

In many cases, including our present problem, before applying the differential quadrature method, one needs to integrate by parts few integrals and then make use of the assumed boundary conditions to rewrite the integral terms. As example, the mid-plane stretching term in Eq. (40), can be re-written after an integration by part as

$$\int_{x=0}^{x=1}\left(\frac{\partial w}{\partial x}\right)^2 dx = \int_0^1 \left(\frac{\partial w}{\partial x}\right)\left(\frac{\partial w}{\partial x}\right) dx = \underbrace{\left[w\frac{\partial w}{\partial x}\right]_{x=0}^{x=1}}_{=0} - \int_0^1 \frac{\partial^2 w}{\partial x^2} w dx \tag{47}$$

Then, this integral can be approximated using the Newton-Cotes formula as follows [49]:

$$\int_0^1 w'' w dx = \sum_{i=1}^{n} C_i w_i'' w_i C_i = \left(\int_0^1 \prod_{k=1,k\neq i}^{n} \frac{x-x_k}{x_i-x_k} dx\right) \tag{48}$$

It is worth mentioning that the above integral is discretized using the same set of grid points as defined previously in Eq. (43). Next, applying the integral approximation as well as the DQM differentiation scheme, Eq. (39) is reduced to the following form:

$$\begin{aligned}
&\left(\ddot{w}_i - \mu_0 \sum_{j=1}^{n} D_{ij}^{(2)} \ddot{w}_j\right) + \left(\sum_{j=1}^{n} D_{ij}^{(4)} w_j - \mu_s \sum_{j=1}^{n} D_{ij}^{(6)} w_j\right) + \alpha_d \left(\dot{w}_i - \mu_0 \sum_{j=1}^{n} D_{ij}^{(2)} \dot{w}_j\right) + \\
&-\alpha_r \left(\sum_{j=1}^{n} D_{ij}^{(2)} \ddot{w}_j - \sum_{j=1}^{n} D_{ij}^{(4)} \ddot{w}_j\right) + \alpha_s \left(\sum_{j=1}^{n}\sum_{k=1}^{n} C_j D_{ij}^{(2)} w_j w_k\right)\left(\sum_{j=1}^{n} D_{ij}^{(2)} w_j - \mu_0 \sum_{j=1}^{n} D_{ij}^{(4)} w_j\right) = \\
&+\mu_k \left(2\sum_{j=1}^{n} D_{ij}^{(2)} \ddot{w}_j - \alpha_r \sum_{j=1}^{n} D_{ij}^{(4)} \ddot{w}_j\right) + \alpha_e \left(\Gamma\left(w_i\right) - \mu_0 \Gamma_{,xx}\left(w_i\right)\right), i = 4, 2, ..., n-3
\end{aligned} \tag{49}$$

Then, to get the total n-equations, the boundary conditions (40) can be used which can be expressed as follows:

$$w_1 = w_n = 0 \sum_{j=1}^{n} D_{1j}^{(1)} w_j = \sum_{j=1}^{n} D_{nj}^{(1)} w_j = 0 \sum_{j=1}^{n} D_{1j}^{(2)} w_j = \sum_{j=1}^{n} D_{nj}^{(2)} w_j = 0 \tag{50}$$

4.2 DQM Formulation for Static Analysis

In this work, we propose to study the effect of varying the nonlocal, the strain gradient and the velocity gradient parameters on the CNT based nano-actuator performance when a static DC voltage is applied. To get the nano-actuator response w_s under a DC voltage, the time-dependent terms in Eqs. (49) and (50) are eliminated. Therefore, the static behavior of the carbon nanotube is given by

$$\begin{aligned}
&\left(\sum_{j=1}^{n} D_{ij}^{(4)} w_{sj} - \mu_s \sum_{j=1}^{n} D_{ij}^{(6)} w_{sj}\right) + \alpha_s \left(\sum_{j=1}^{n}\sum_{k=1}^{n} C_j D_{ij}^{(2)} w_{sj} w_{sk}\right)\left(\sum_{j=1}^{n} D_{ij}^{(2)} w_{sj} - \mu_0 \sum_{j=1}^{n} D_{ij}^{(4)} w_{sj}\right) = \\
&\alpha_r \left(\sum_{j=1}^{n} D_{ij}^{(2)} \ddot{w}_{sj} - \sum_{j=1}^{n} D_{ij}^{(4)} \ddot{w}_{sj}\right) + \alpha_e \left(\Gamma\left(w_{si}\right) - \mu_0 \Gamma_{,xx}\left(w_{si}\right)\right), i = 4, 2, ..., n-3
\end{aligned} \tag{51}$$

$$w_{s1} = w_{sn} = 0 \sum_{j=1}^{n} D_{1j}^{(1)} w_{sj} = \sum_{j=1}^{n} D_{nj}^{(1)} w_{sj} = 0 \sum_{j=1}^{n} D_{1j}^{(2)} w_{sj} = \sum_{j=1}^{n} D_{nj}^{(2)} w_{sj} = 0 \tag{52}$$

Consequently, the equations are reduced to n-algebraic nonlinear equations that can be solved numerically for the discretized static points w_{si} for $i = 1, .., n$.

4.3 DQM Formulation for Eigenvalue Analysis

In this section, we study the variation of the natural frequencies of the carbon nanotube actuator with various nonlocal-parameter, strain gradient and velocity gradient levels under a static DC voltage actuation. Toward this, we consider the DQM discretized equations obtained in Eqs. (49) and (50), which can be re-arranged in a matrix form as:

$$LHS\,(w)\,\dot{w} = RHS\,(w) \tag{53}$$

where $w = [w_1, w_2, w_3,...,w_n,\dot{w}_1,\dot{w}_2,\dot{w}_3,...,\dot{w}_n]$ is the carbon nanotube deflection discretized DQM points vector, $LHS\,(w)$ is a nonlinear matrix representing the right-hand side coefficients multiplying the vector $\dot{w}$ and $RHS\,(w)$ is a right-hand side vector representing the forcing, stiffness, and damping coefficients. Both $LHS\,(w)$ and $RHS\,(w)$ are nonlinear functions of the discretized nanotube deflection w_i. Next, we split w into a static component w_s, representing the equilibrium position due to the DC static actuation, and a dynamic component w_m, representing the perturbation around the equilibrium position, that is

$$w = w_s + w_d \tag{54}$$

Next, substituting (54) into (53), using an expansion based on a Taylor series while assuming small w_d, neglecting the higher-order terms and using the fact that $RHS\,(w_s) = 0$, we obtain the following linearized equation:

$$LHS\,(w_s)\,\dot{w}_d = \nabla RHS\,(w_s)\,w_d + \underbrace{HOT}_{=0} \tag{55}$$

where $\nabla RHS\,(w_s)$ is the gradient of the right-hand matrix evaluated at the equilibrium static points w_s. To determine the natural frequencies of the nano-actuator, we substitute the stable static solution w_s into the Jacobian matrix defined as

$$J = LHS^{-1} \nabla RHS \tag{56}$$

The eigenvalues λ of the jacobian matrix can be calculated by solving the following characteristic algebraic equation:

$$\det\left(J\,(w_s) - \lambda I\right) = 0 \tag{57}$$

in which I is the identity matrix. Finally, the natural frequencies of the system are obtained by taking the square-root of each individual eigenvalue.

5 Numerical Results and Discussion

Two separate cases of carbon nanotubes are considered for simulation purposes in this paper, both of which are summarized in Table 1. We have shown in a previous investigation that using 11 discretization points in the DQM is enough to capture the response of a CNT and assure convergence [50]. But since here we had to deal with few more boundary conditions (two non-classical boundary conditions), we decided to use 19 points in the DQM.

Table 1: Geometrical properties of the considered carbon nanotubes in this investigation

Case No.	d [nm]	L [nm]	$\tilde{R}$ [nm]	Reference
1	4	50	0.678	[35]
2	100	3000	30	[51]

5.1 Results Validation

In order to validate the formulation presented in this paper, a carbon nanotube of case 2 of Table 1 is studied. The DC voltage is used for different values of the nonlocal parameter $\mu_0 = 0$ and 0.2^2 and the strain and velocity gradient parameters $\mu_s = \mu_k = 0$. Fig. 2 shows the variation of the normalized maximum static deflection for carbon nanotube of case 2 of Table 1 as a function of the DC voltage. The results show excellent agreement with those reported in [35].

5.2 Parametric Study

In this section, a number of examples are studied to demonstrate the effectiveness of the proposed formulation to predict the response of CNT nanobeams.

The first example consists of the carbon nanotube of case 1 of Table 1 with zero DC voltage. To illustrate the effect of the internal length scales, variation of the normalized higher-order frequencies versus three internal lengths (including nonlocal parameter, strain gradient parameter, and velocity gradient parameter) are plotted in Figs. 3a, 3b, and 3c). The first three natural frequencies are illustrated in each of these figures. It is observed that higher values of nonlocal parameter and velocity gradient parameter results in a reduction of the frequencies. In contrast, by increasing the strain gradient parameter, the frequencies are increasing.

In the second example, the effect of the DC voltage is investigated. For the carbon nanotube corresponding to case 2 of Table 1, Figs. 4a and 4b) show the variation of the normalized frequencies with the nonlocal parameter for zero DC voltage and 6 Volt DC voltage, respectively. It is observed that the first frequency of the latter possesses a maximum in contrast to the case of zero DC voltage. It is also interesting to note that when a DC voltage is applied, a cross-over of the first two natural frequencies for a value of the nonlocal parameter equal to about 0.15 as shown in Fig. 4b in which the second mode of vibration becomes the fundamental mode.

Next example addresses the effect of the nonlocal parameter on the maximum static deflection as a function of the DC voltage, while it is assumed that $\mu_s = \mu_k = 0$. For the carbon nanotube of case 1 of Table 1, the normalized maximum static deflection versus the

DC voltage is plotted in Fig. 5. The results show that higher values of nonlocal parameter lead to lower deflection and higher pull-in voltage indicating that the CNT beam becomes stiffer due essentially to variation of the effective nonlinear stiffness. Furthermore, increasing the DC voltage results evidently in higher deflection.

As a fourth example, the variation of the fundamental, second and third frequencies in terms of the DC voltage are plotted separately to look into the effect of nonlocal parameter while $\mu_s = \mu_k = 0$. As shown in Figs. 6a, 6b, and 6c, for the carbon nanotube of case 1 of Table 1, the qualitative behavior of the second and third frequencies are somehow analogous, nevertheless dissimilar as compared to the first frequency. In reality, the fundamental first frequency shows a minor decline followed by an rise when increasing the assumed DC load before the manifestation of the pull-in instability (the first frequency drops to zero). It is also worth mentioning that increasing the nonlocal parameter values tends to decrease this fundamental first frequency up to a DC load of about 40 volts and then an contrasting outcome is experienced furthermore with a noticeable increase of the pull-in voltage. Moreover, when the nonlocal parameter increases, the second and third frequencies are decreased.

The variation of the normalized maximum static deflection for the carbon nanotube of case 1 of Table 1 with the DC voltage is plotted in Fig. 7. Three different values of the strain gradient parameter $\mu_s = 0$, 0.1^2 and 0.2^2 with $\mu_s = \mu_k = 0$ are considered here. It is observed that the deflection increases with voltage but decreases by increasing the strain gradient parameter. Furthermore, comparing Figs. 5) and (7 indicates that the nonlocal and strain gradient parameters have a similar overall effect but the effect of the latter parameter is more prominent.

Considering a carbon nanotube of case 1 of Table 1, in the next example (Figs. 8a, 8b, and 8c), the variation of the normalized fundamental, second and third frequency with the DC voltage are illustrated for three different values of the strain gradient parameter $\mu_s = 0$, 0.1^2 and 0.2^2 together with $\mu_s = \mu_k = 0$. Similar to example four, the fundamental frequency exhibits qualitatively different behavior in comparison to the second and third frequencies. Increasing the values of the strain gradient parameter leads to an increase in the frequencies and in addition to a further growth of the pull-in voltage. This effect is opposite to that of the nonlocal parameter.

For the carbon nanotube of case 1 of Table 1, the variation of the normalized fundamental, second, and third frequencies versus the DC voltage are plotted in Figs. 9a, 9b, and 9c for three different values of the velocity gradient parameter $\mu_k = 0$, 0.1^2 and 0.2^2 with $\mu_0 = \mu_s = 0$. Again the fundamental frequency possesses a maximum value in contrast to the other frequencies. Moreover, increasing the values of the velocity gradient parameter leads to a decrease in the frequencies.

The final example considers simultaneous changes to the nonlocal parameters for fixed DC voltage, and the results are shown in Fig. 10. It is clear that the fundamental natural frequency reduces with μ_k (softening effect) and increases with μ_s (hardening effect). For low values of μ_k the fundamental natural frequency reduces with μ_0. However for high values of μ_k the natural frequency increases with μ_0 for low values of μ_s and reduces for high values of μ_s; hence in this range of parameters the softening and hardening effects approximately cancel.

6 Conclusions

The static and dynamic nonlinear responses of an electrically actuated CNT based nano-actuator was investigated using a nonlocal strain and velocity strain gradient theory. The nano-actuator was modeled as a clamped-clamped Euler-Bernoulli beam with von Karman strain nonlinearity. The principle of Hamilton was employed to establish the nonlinear governing equation of motion of the CNT based nano-actuator along with its respective classical/non-classical boundary conditions. The differential quadrature discretization technique was then employed to discretize the nonlinear equation of motion yielding nonlinear static and free vibration equations.

The nonlocal parameter and the strain gradient parameters influences on the static response was first examined. It was concluded that any rise of both parameters result into a growth in the effective forcing on the CNT causing an apparent reduction in the beam overall stiffness, which in turn reduces the static response and enlarges the pull-in voltage. The free vibration response was obtained by linearizing the eigenvalue problem around the static solution and the natural frequencies of the nano-beam were then computed. It was shown that for a zero actuating load, any increase of the nonlocal parameter reduces all natural frequencies up to the third mode. When a DC voltage is applied, the fundamental frequency is first slightly decreased and then increased due to the hardening behavior of the quadratic nonlinearity of the electrostatic force before dropping to zero at the pull-in instability. The second and third frequencies exhibit an increase as a function of the applied DC voltage and the nonlocal parameter tends to increase the voltage at the pull-in instability. In contrast, it was shown that an increase in the strain gradient parameter increases the fundamental frequency with the electric load. Finally, it was revealed that an increase in the velocity gradient parameter results in a reduction of the fundamental frequency without altering its overall variation pattern with the DC load. The acquired results allow better understanding of the nonlinear behavior of tiny CNT devices and can guide us to improve their overall performance accordingly.

Acknowledgements. The second author is grateful to the support of Texas A&M University at Qatar.

References

[1] V. Sazonova, Y. Yaish, H. Ustunel, D. Roundy, T.A. Arias, P.L. McEuen, A tunable carbon nanotubes electromechanical oscillator, Nature, 431 (2004), 284-287.

[2] H. Ustunel, D. Roundy, and T.A. Arias, Modeling a suspended nanotube oscillator, Nano Letters, 5 (2005), 523-526.

[3] L. Liu, Y. Zhang, Multi-Wall Carbon Nanotube as a New Infrared Detected Material, Sensors and Actuators A, 116 (2004), 394-397.

[4] Y.L. Chen, B. Liu, J. Wu, Y. Huang, H. Jiang, K.C. Hwang, 2008, Mechanics of Hydrogen Storage in Carbon Nanotubes, Journal of Mechanics and Physics of Solids, 56 (2008), 3224-3241.

[5] C. Zhao, Y. Song, J. Ren, X. Qu, 2009, A DNA Nanomachine Induced by Single-Walled Carbon Nanotubes on Gold Surface, Biomaterials, 30 (2009), 1739-1745.

[6] C. Qin, J. Shen, Y. Hu, M. Ye, Facile Attachment of Magnetic Nanoparticles to Carbon Nanotubes Via Robust Linkages and Its Fabrication of Magnetic Nanocomposites, Composite Science Technology, 69 (2009), 427-431.

[7] A.C. Eringen, Nonlocal polar elastic continua, International Journal of Engineering Science 10 (1972), 1-16.
[8] A.C. Eringen, On differential equations of nonlocal elasticity and solutions of screw dislocation and surface waves, Journal of Applied Physics, 54 (1983), 4703-4710.
[9] A.C. Eringen, Nonlocal Continuum Field Theories, Springer-Verlag, New York (2002).
[10] A.C. Eringen, D.G.B. Edelen, On nonlocal elasticity, International Journal of Engineering Science, 10 (1972), 233-248.
[11] R.D. Mindlin, Influence of couple-stresses on stress concentrations, Experimental Mechanics, 3 (1963), 1-7.
[12] W.T. Koiter, Couple-stresses in the theory of elasticity: I and II, Koninklijke Nederlandse Akademie van Wetenschappen (Royal Netherlands Academy of Arts and Sciences) B67 (1964), 17-44.
[13] R.A. Toupin, Theories of elasticity with couple-stress, Archive for Rational Mechanics and Analysis, 17 (1964), 85-112.
[14] R.D. Mindlin, Second gradient of strain and surface-tension in linear elasticity, International Journal of Solids and Structures, 1 (1965), 217-238.
[15] F. Yang, A.C.M. Chong, D.C.C. Lam and P. Tong, Couple stress based strain gradient theory for elasticity, International Journal of Solids and Structures, 39 (2002), 2731-2743.
[16] D.C.C. Lam, F. Yang, A.C.M. Chong, J. Wang, P. Tong, Experiments and theory in strain gradient elasticity, Journal of Mechanics and Physics of Solids, 51 (2003), 1477-1508.
[17] L. Li, Y. Hu, Nonlinear bending and free vibration analyses of nonlocal strain gradient beams made of functionally graded material, International Journal of Engineering Science, 107 (2016), 77-97.
[18] X. Zhu, L. Li, Closed form solution for a nonlocal strain gradient rod in tension, International Journal of Engineering Science, 119 (2017) 16-28.
[19] Y. Tian, B. Xu, D. Yu, Y. Ma, Y. Wang, Y. Jiang, Ultrahard nanotwinned cubic boron nitride. Nature, 493 (2013), 385-388.
[20] H. Askes, E.C. Aifantis, Gradient elasticity in statics and dynamics: An overview of formulations, length scale identification procedures, finite element implementations and new results. International Journal of Solids and Structures, 48:13 (2011), 1962-1990 .
[21] C.W. Lim, G. Zhang, J.N. Reddy, A higher-order nonlocal elasticity and strain gradient theory and its applications in wave propagation. Journal of the Mechanics and Physics of Solids, 78 (2015), 298-313.
[22] C. Thongyothee, S. Chucheepsakul, T. Li, Nonlocal elasticity theory for free vibration of single-walled carbon nanotubes, Advanced Materials Research, 747 (2013), 257-260.
[23] K. Kiani, Vibration behavior of simply supported inclined single-walled carbon nanotubes conveying viscous fluids flow using nonlocal Rayleigh beam model, Applied Mathematical Modelling, 37-4 (2013), 1836-1850.
[24] X.-J. Xu, Z.-C. Deng, Variational principles for buckling and vibration of MWCNTs modeled by strain gradient theory, Applied Mathematics and Mechanics, 35 (2014), 1115-1128.
[25] L. Li, H. Yujin, L. Xiaobai, Longitudinal vibration of size-dependent rods via nonlocal strain gradient theory, International Journal of Mechanical Sciences, 115 (2016), 135-144.
[26] M.A. De Rosa, M. Lippiello, Nonlocal Timoshenko frequency analysis of single-walled carbon nanotube with attached mass: An alternative hamiltonian approach, Compos-

ites Part B, 111 (2017), 409-418.
[27] R. Ansari, R. Gholami, S. Ajori, Torsional vibration analysis of carbon nanotubes based on the strain gradient theory and molecular dynamic simulations, Journal of Vibration and Acoustics, 135-5 (2013), 051016.
[28] M.M.S. Fakhrabadi, A. Rastgoo, M.T. Ahmadian, M. Mosavi Mashhadi, Dynamic analysis of carbon nanotubes under electrostatic actuation using modified couple stress theory, Acta Mechanica, 225-6 (2014), 1523-1535.
[29] I. Mehdipour, A. Erfani-Moghadam, C. Mehdipour, Application of an electrostatically actuated cantilevered carbon nanotube with an attached mass as a bio-mass sensor, Current Applied Physics, 13-7 (2013), 1463-1469.
[30] B. Fang, Y.-X. Zhen, C.-P. Zhang, Y. Tang, Nonlinear vibration analysis of double-walled carbon nanotubes based on nonlocal elasticity theory, Applied Mathematical Modelling, 37 (2013), 1096-1107.
[31] L.-L. Ke, J. Yang, S. Kitipornchai, Nonlinear free vibration of functionally graded carbon nanotube-reinforced composite beams, Composite Structures, 92-3 (2010), 676-683.
[32] J. Yang, L.-L. Ke, S. Kitipornchai, Nonlinear free vibration of single-walled carbon nanotubes using nonlocal Timoshenko beam theory, Physica E: Low-dimensional Systems and Nanostructures, 5 (2010), 1727-1735.
[33] L.-L. Ke, Y. Xiang, J. Yang, S. Kitipornchai, Nonlinear free vibration of embedded double-walled carbon nanotubes based on nonlocal Timoshenko beam theory, Computational Materials Science, 47 (2009), 409-417.
[34] M. Rahmanian, M.A.Torkaman-Asadi, R.D.Firouz-Abadi, M.A.Kouchakzadeh, Free vibrations analysis of carbon nanotubes resting on Winkler foundations based on nonlocal models, Physica B: Condensed Matter 484 (2016), 83-94.
[35] P. Ribeiro, Non-local effects on the nonlinear modes of vibration of carbon nanotubes under electrostatic actuation, International Journal of Non-Linear Mechanics, 87 (2016), 1-20.
[36] W.D. Yang, F.P. Yang, X. Wang, Coupling influences of nonlocal stress and strain gradients on dynamic pull-in of functionally graded nanotubes reinforced nano-actuator with damping effects, Sensors and Actuators A: Physical, 248 (2016), 10-21.
[37] R.D. Mindlin, Micro-structure in linear elasticity, Archive for Rational Mechanics and Analysis, 16-1 (1964), 51-78.
[38] G. Rosi, L. Placidi, N. Auffray, On the validity range of strain-gradient elasticity: a mixed static-dynamic identification procedure, European Journal of Mechanics-A/Solids, 69 (2018), 179-191.
[39] S. Guo, Y. He, D. Liu and J. Lei, L. Shen, Z. Li, Torsional vibration of carbon nanotube with axial velocity and velocity gradient effect, International Journal of Mechanical Sciences, 119 (2016), 88-96.
[40] R. Fernandes, S. El-Borgi, S.M. Mousavi, J.N. Reddy, A. Mechmoum, Nonlinear size-dependent longitudinal vibration of carbon nanotubes embedded in an elastic medium, Physica E: Low-dimensional Systems and Nanostructures, 88 (2017), 18-25.
[41] R. Fernandes, S.M. Mousavi, S. El-Borgi, Free and forced vibration nonlinear analysis of a microbeam using finite strain and velocity gradients theory, Acta Mechanica, 227-9 (2016), 2657-2670.
[42] S. El-Borgi, P. Rajendran, M.I. Friswell, M. Trabelssi, J.N. Reddy, Torsional vibration of size-dependent viscoelastic rods using nonlocal strain and velocity gradient theory, Composite Structures, 186 (2018), 274-292.

[43] M.F. Yu, Fundamental mechanical properties of carbon nanotubes: current understanding and the related experimental studies?, Journal of Engineering Materials and Technology, 126 (2004), 271-278.

[44] A.C. Eringen, Linear theory of nonlocal elasticity and dispersion of plane waves, International Journal of Engineering Science, 10-5 (1972), 425-435.

[45] C.W. Lim, C.M. Wang, Exact variational nonlocal stress modeling with asymptotic higher-order strain gradients for nanobeams, Journal of Applied Physics, 101-5 (2007), 054312.

[46] J. Fernández-Sáez, R. Zaera, J.A. Loya, J.N. Reddy. Bending of Euler-Bernoulli beams using Eringen's integral formulation: a paradox resolved, International Journal of Engineering Science, 99 (2016) 107-116.

[47] G. Romano, R. Barretta, M. Diaco, F. Marotti de Sciarra, Constitutive boundary conditions and paradoxes in nonlocal elastic nanobeams, International Journal of Mechanical Sciences, 121 (2017) 151-156.

[48] R.D. Mindlin, Micro-structure in linear elasticity, Archive for Rational Mechanics and Analysis, 16-1 (1964), 51-78.

[49] S. Tomasiello, Differential Quadrature Method: Application to Initial-Boundary-Value Problems, Journal of Sound and Vibration, 218-4 (1998), 573-585.

[50] H.M. Ouakad, F. Najar , O. Hattab, Nonlinear Analysis of Electrically Actuated Carbon Nanotube Resonator Using a Novel Discretization Technique, Mathematical Problems in Engineering, (2013), Article ID 517695, 9 pages.

[51] H.M. Ouakad, M.I. Younis, Nonlinear dynamics of electrically actuated carbon nanotube resonators, Journal of Computational and Nonlinear Dynamics, 5-1 (2010), 011009.

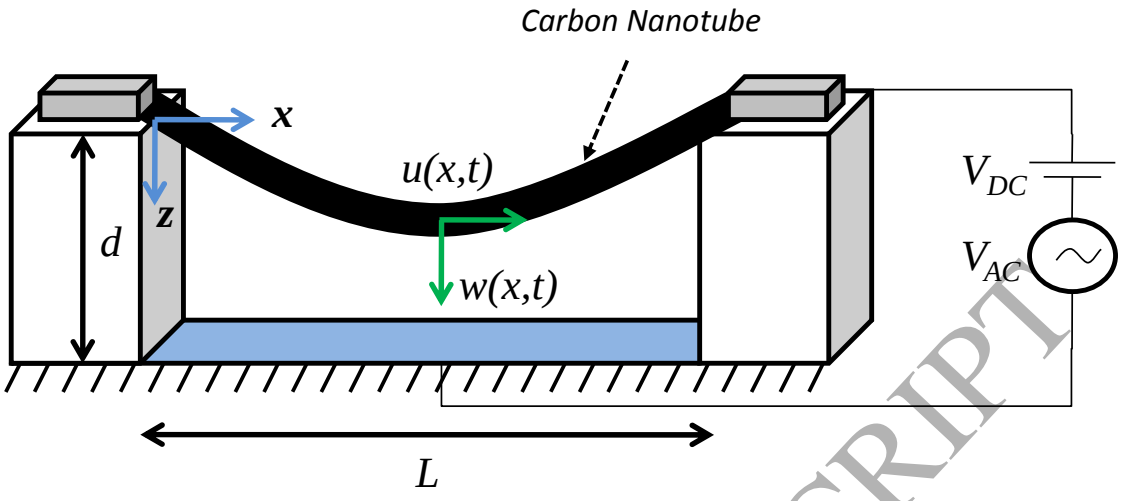

Fig. 1: Schematic of an electrically actuated clamped-clamped carbon nanotube based NEMS resonator.

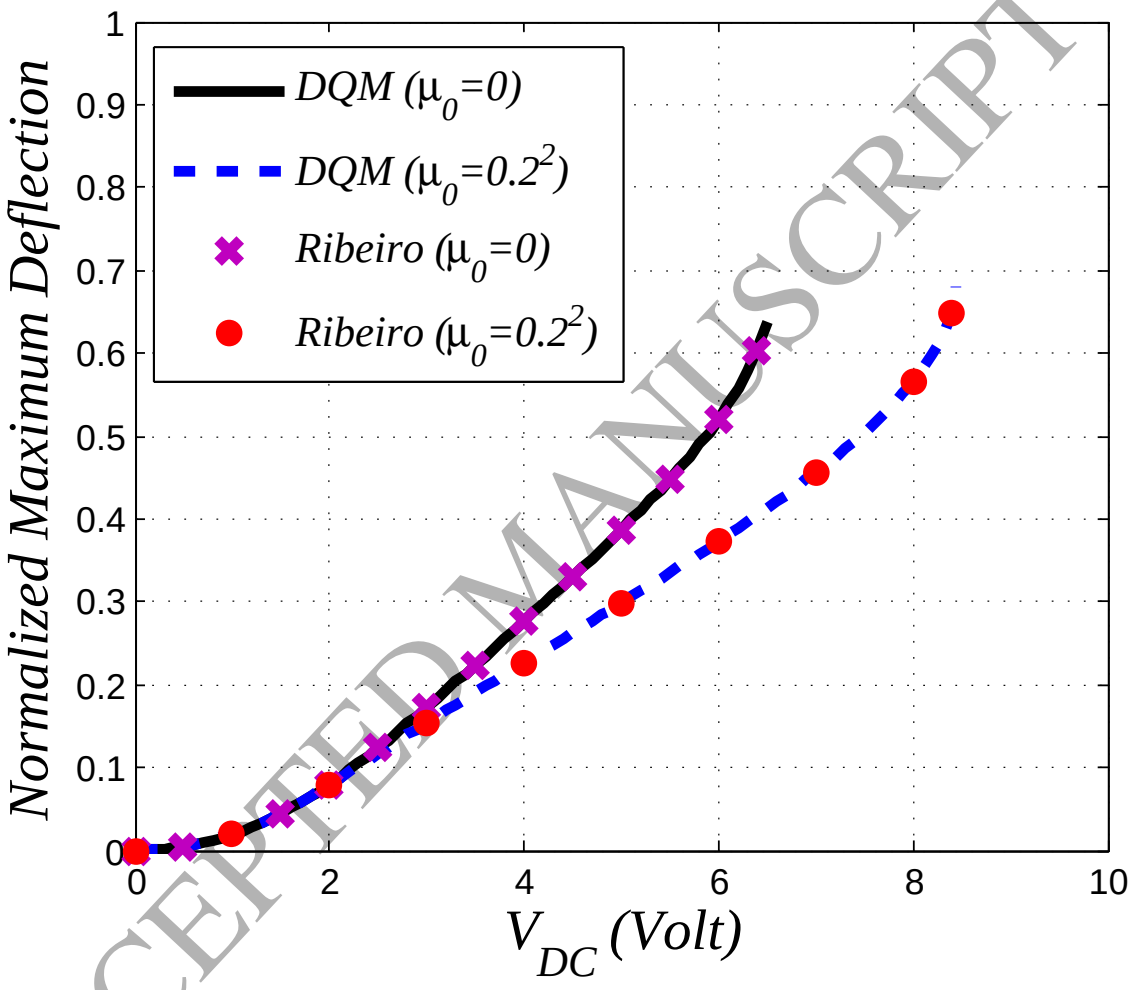

Fig. 2: Variation of the normalized maximum static deflection for carbon nanotube of case 2 of Table 1 with the DC voltage and for different values of the nonlocal parameter and $\mu_s = \mu_k = 0$. In the figure: (?) and (x) are the results reported in [35].

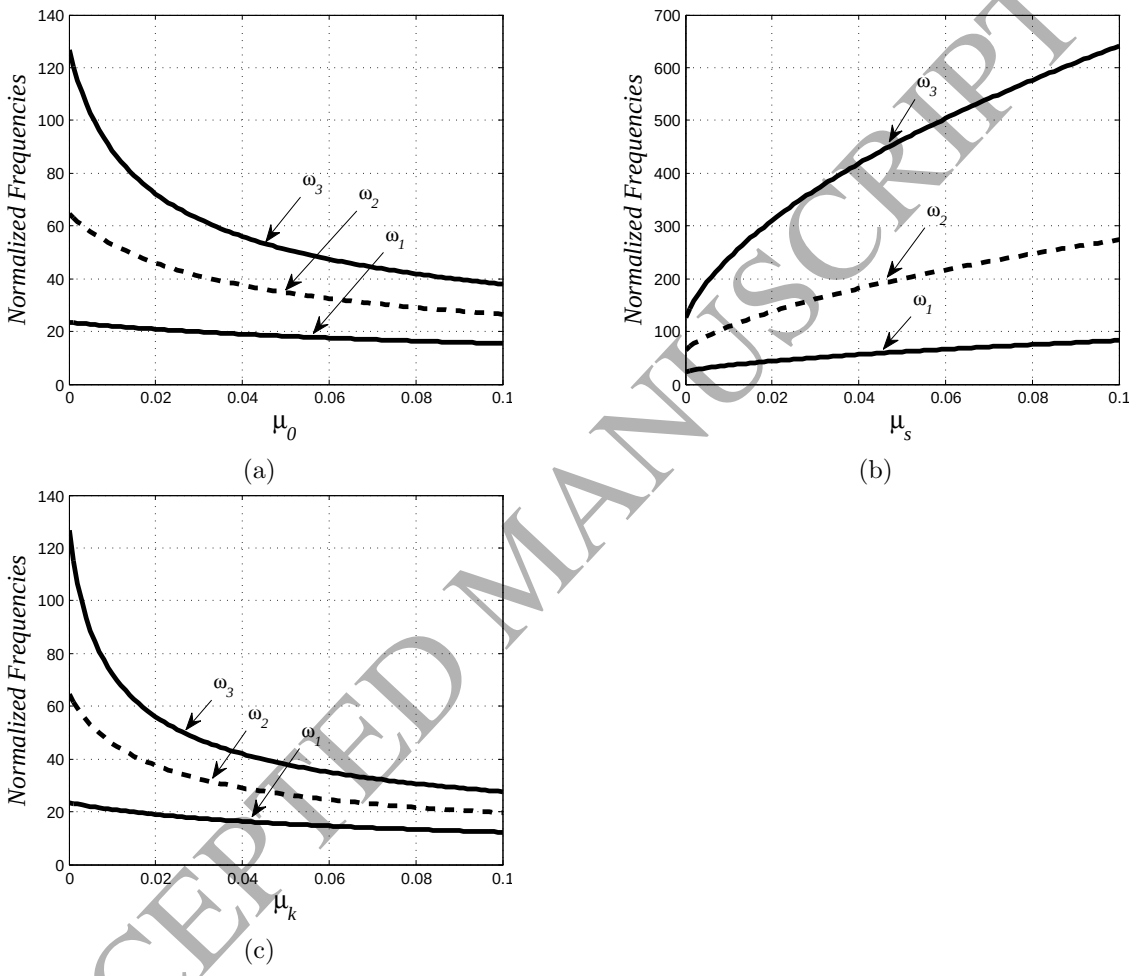

Fig. 3: Variation of the normalized higher-order frequencies for the carbon nanotube of case 1 of Table 1 with the (a) nonlocal parameter, (b) strain gradient parameter, and (c) velocity gradient parameter for zero DC voltage.

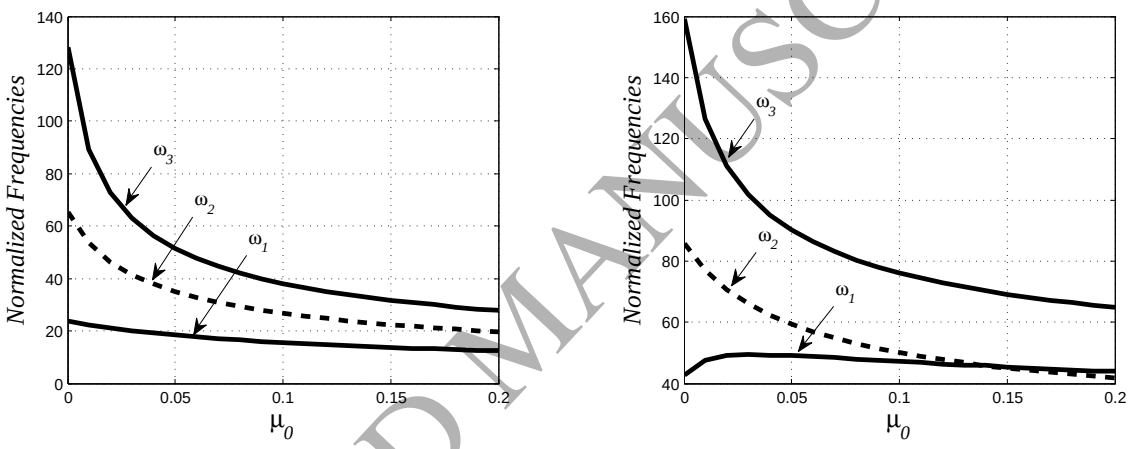

Fig. 4: Variation of the normalized higher-order frequencies for the carbon nanotube of case 2 of Table 1 with the nonlocal parameter, and for (a) zero DC voltage, and (b) 6 Volt DC voltage.

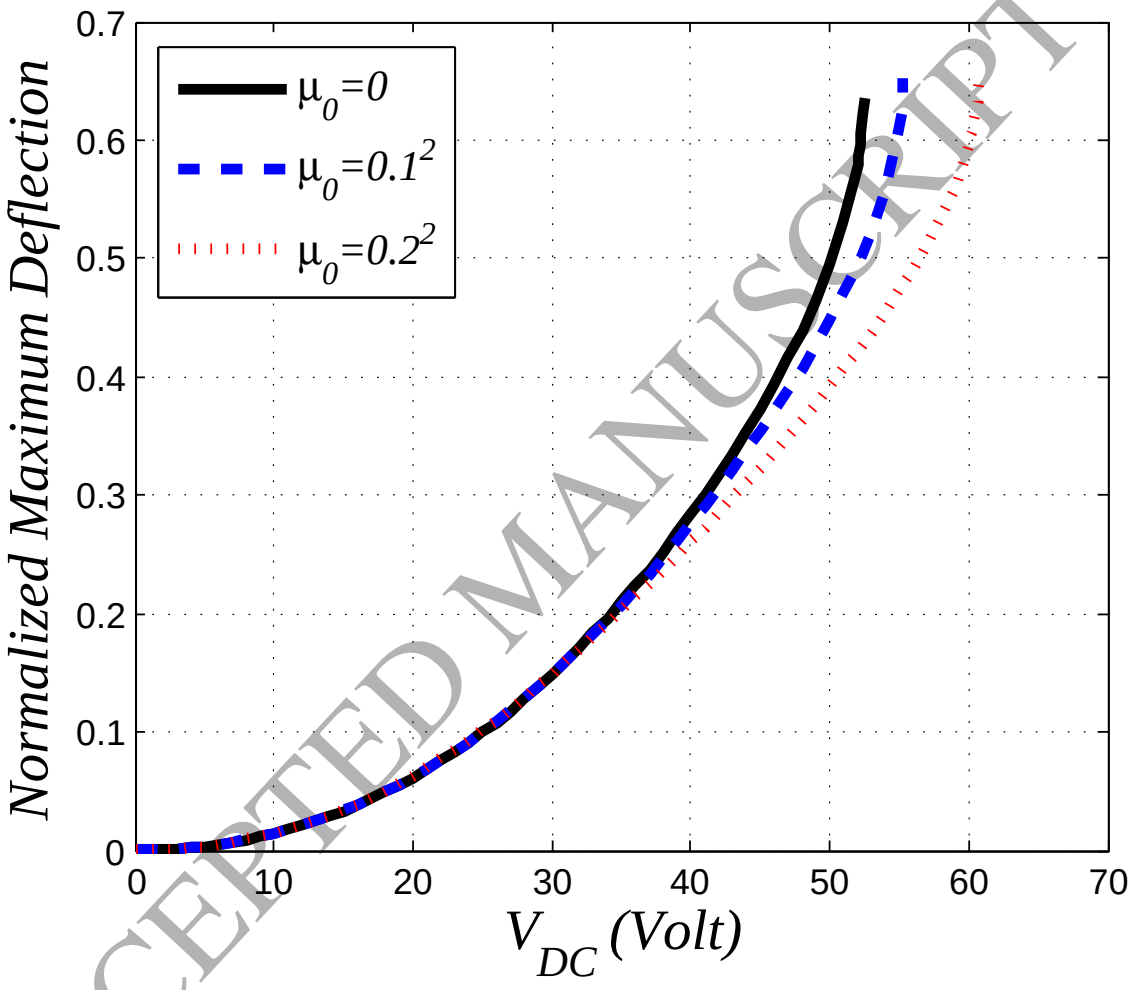

Fig. 5: Variation of the normalized maximum static deflection for the carbon nanotube of case 1 of Table 1 with the DC voltage and for different values of the nonlocal parameter and $\mu_s = \mu_k = 0$.

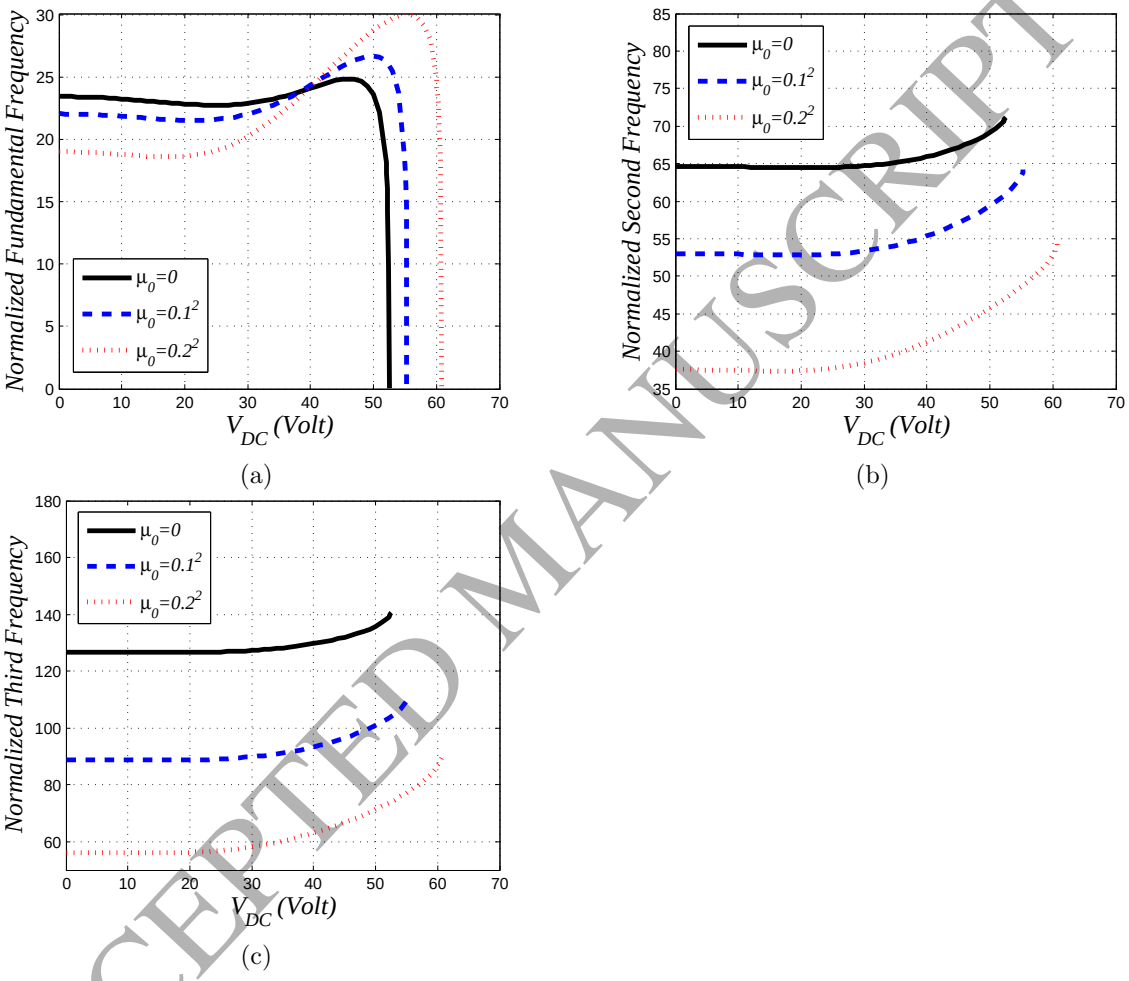

Fig. 6: Variation of the normalized (a) fundamental frequency, (b) second frequency, and (c) third frequency, for the carbon nanotube of case 1 of Table 1 with the DC voltage and for different values of the nonlocal parameter and $\mu_s = \mu_k = 0$.

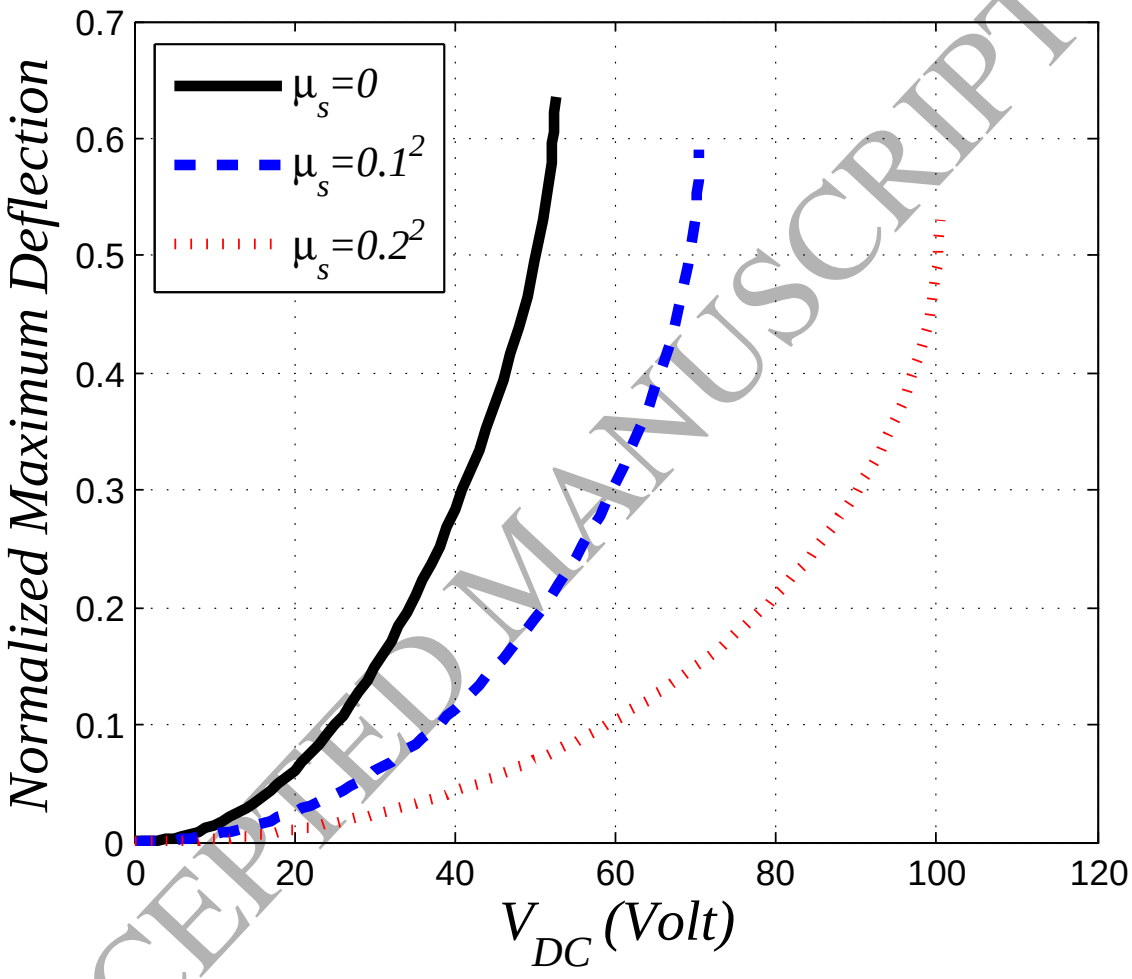

Fig. 7: Variation of the normalized maximum static deflection for the carbon nanotube of case 1 of Table 1 with the DC voltage and for different values of the strain gradient parameter $\mu_s = 0; 0.1^2; 0.2^2$ and for $\mu_0 = \mu_k = 0$.

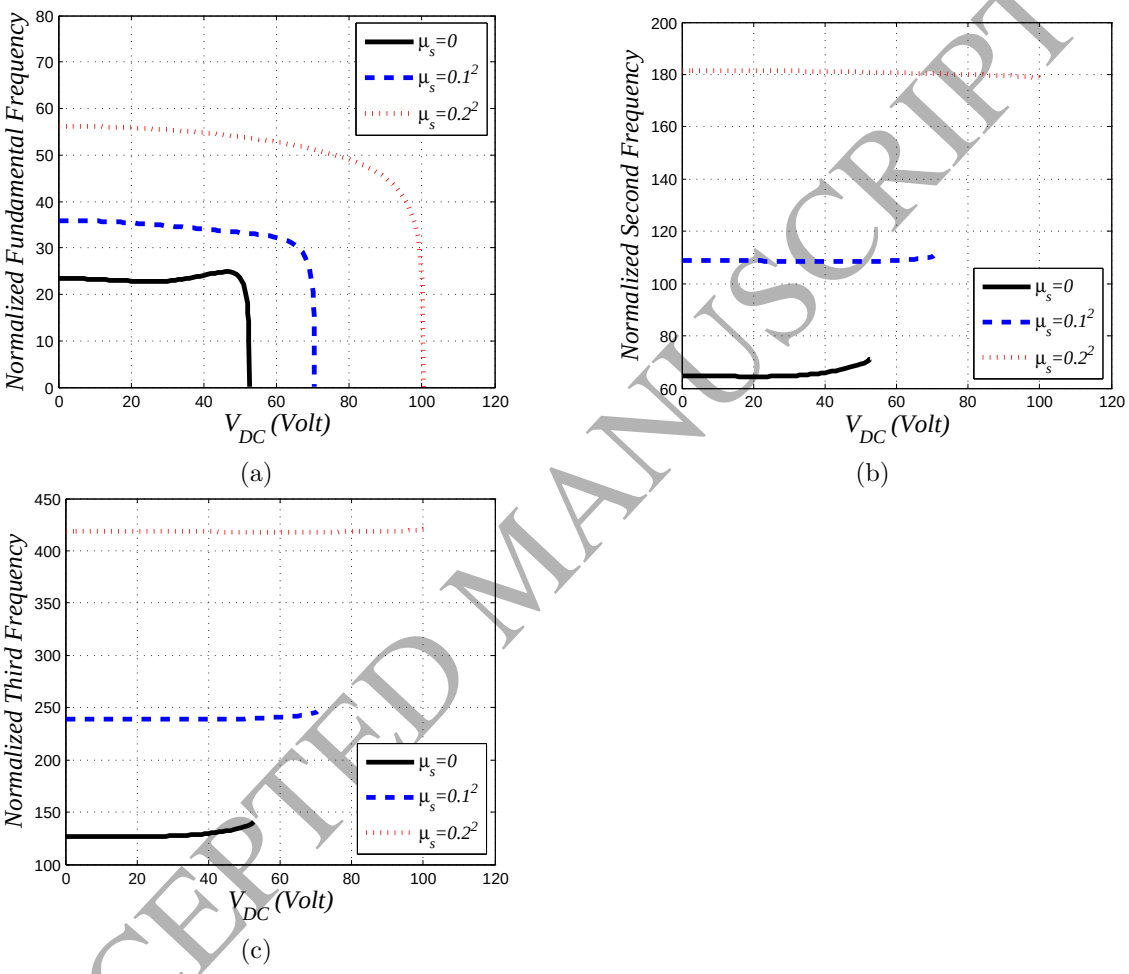

Fig. 8: Variation of the normalized (a) fundamental frequency, (b) second frequency, and (c) third frequency, for the carbon nanotube of case 1 of Table 1 with the DC voltage and for different values of the strain gradient parameter $\mu_s = 0; 0.1^2; 0.2^2$ and for $\mu_0 = \mu_k = 0$.

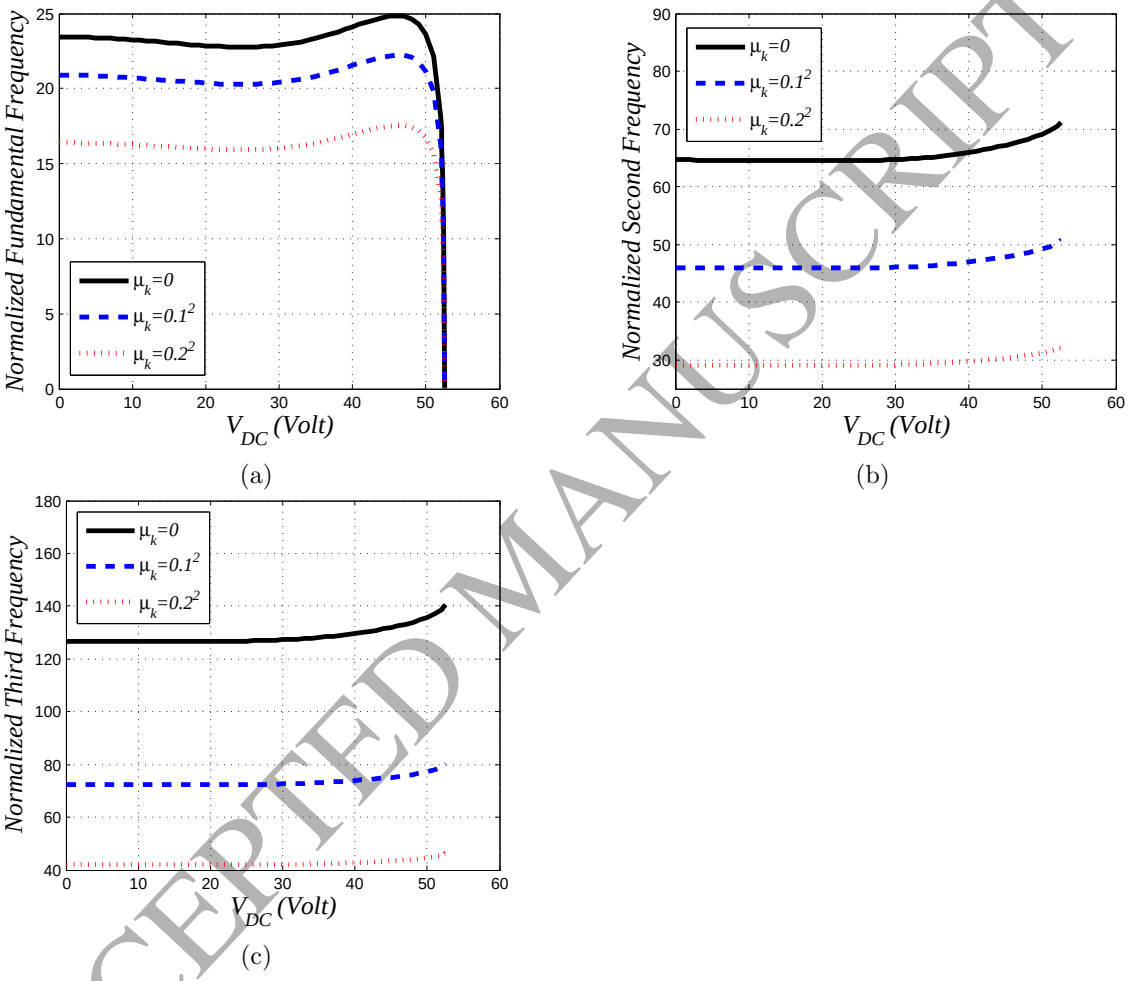

Fig. 9: Variation of the normalized (a) fundamental frequency, (b) second frequency, and (c) third frequency, for the carbon nanotube of case 1 of Table 1 with the DC voltage and for different values of the velocity gradient parameter $\mu_k = 0; 0.1^2; 0.2^2$ and for $\mu_0 = \mu_s = 0$.

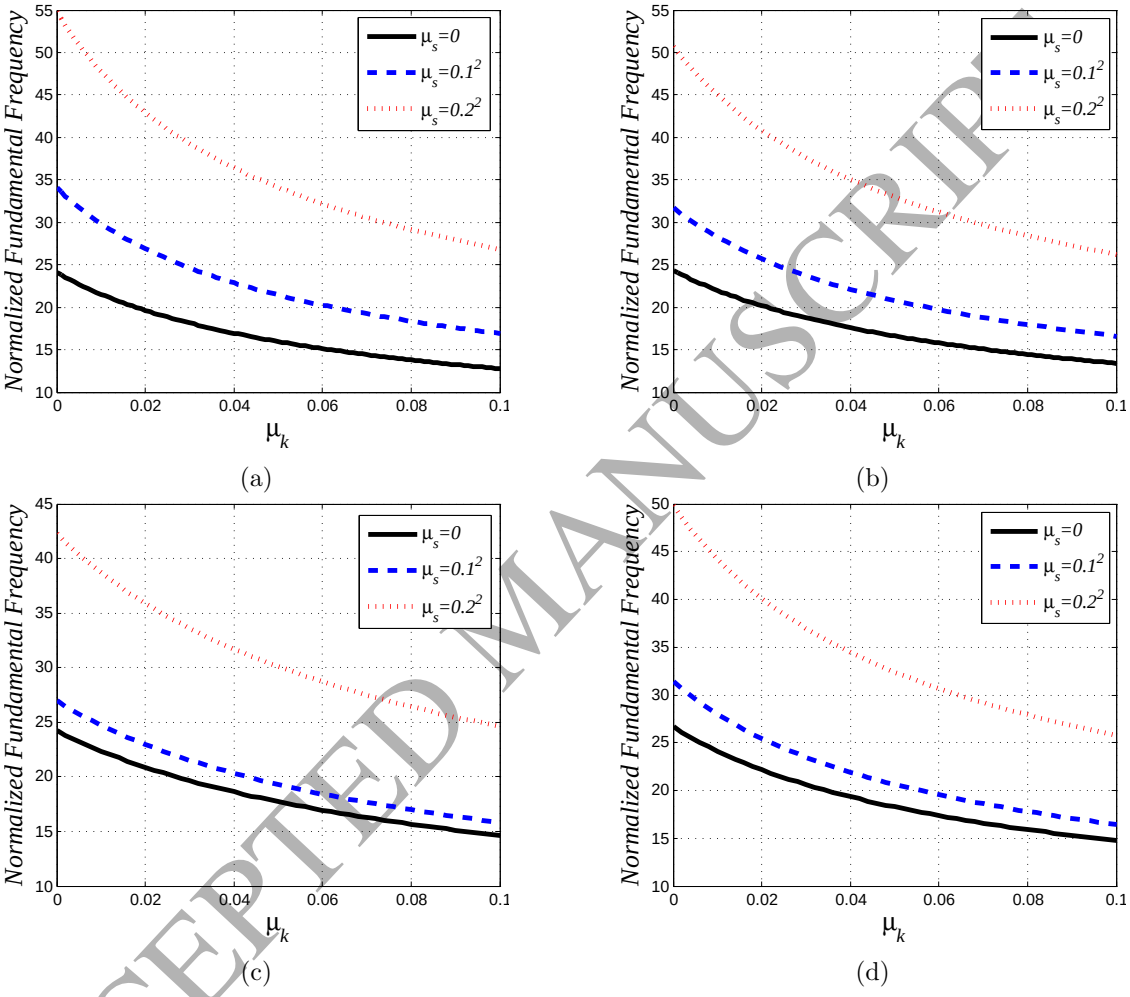

Fig. 10: Variation of the normalized fundamental frequency as a function of the velocity gradient parameter, μ_k, for different values of the strain gradient parameter $\mu_s = 0; 0.1^2; 0.2^2$ and for fixed values of the DC voltage, V_{DC}, and nonlocal parameter, μ_0 (a) $V_{DC} = 40V$ and $\mu_0 = 0$; (b) $V_{DC} = 40V$ and $\mu_0 = 0.1^2$; (c) $V_{DC} = 40V$ and $\mu_0 = 0.2^2$; (d) $V_{DC} = 50V$ and $\mu_0 = 0.1^2$.